ELSEVIER

8 May 1997

PHYSICS LETTERS B

Physics Letters B 400 (1997) 226–238

A search for axial vectors in $\bar{p}p \to K^{\pm}K^{0}_{\rm miss}\pi^{\mp}\pi^{+}\pi^{-}$ annihilations at rest in gaseous hydrogen at NTP

OBELIX Collaboration

A. Bertin [a], M. Bruschi [a], M. Capponi [a], A. Collamati [a], S. De Castro [a], R. Donà [a], A. Ferretti [a], D. Galli [a], B. Giacobbe [a], U. Marconi [a], M. Piccinini [a], N. Semprini-Cesari [a], R. Spighi [a], S. Vecchi [a], A. Vezzani [a], F. Vigotti [a], M. Villa [a], A. Vitale [a], A. Zoccoli [a], M. Corradini [b], A. Donzella [b], E. Lodi Rizzini [b], L. Venturelli [b], A. Zenoni [c], C. Cicaló [d], A. Lai [d], A. Masoni [d], L. Musa [d], G. Puddu [d], S. Serci [d], P.P. Temnikov [d,1], G. Usai [d], O.E. Gorchakov [e], S.N. Prakhov [e], A.M. Rozhdestvensky [e], M.G. Sapozhnikov [e], V.I. Tretyak [e], M. Poli [f], P. Gianotti [g], C. Guaraldo [g], A. Lanaro [g], V. Lucherini [g], F. Nichitiu [g,2], C. Petrascu [g,2], A. Rosca [g,2], V. Ableev [h], C. Cavion [h], U. Gastaldi [h], M. Lombardi [h], G. Maron [h], L. Vannucci [h], G. Vedovato [h], G. Bendiscioli [i], V. Filippini [i], A. Fontana [i], P. Montagna [i], A. Rotondi [i], A. Saino [i], P. Salvini [i], C. Scoglio [i], F. Balestra [j], E. Botta [j], T. Bressani [j], M.P. Bussa [j], L. Busso [j], D. Calvo [j], P. Cerello [j], S. Costa [j], O. Denisov [j,1], L. Fava [j], A. Feliciello [j], L. Ferrero [j], A. Filippi [j], R. Garfagnini [j], A. Grasso [j], A. Maggiora [j], S. Marcello [j], D. Panzieri [j], D. Parena [j], E. Rossetto [j], F. Tosello [j], L. Valacca [j], M. Agnello [k], F. Iazzi [k], B. Minetti [k], G. Pauli [ℓ], S. Tessaro [ℓ], L. Santi [m]

[a] *Dipartimento di Fisica, Università di Bologna and INFN, Sezione di Bologna, Bologna, Italy*
[b] *Dipartimento di Chimica e Fisica per i Materiali, Università di Brescia and INFN, Sezione di Torino, Torino, Italy*
[c] *Dipartimento di Chimica e Fisica per i Materiali,, Università di Brescia and INFN, Sezione di Pavia, Pavia, Italy*
[d] *Dipartimento di Scienze Fisiche, Università di Cagliari and INFN, Sezione di Cagliari, Cagliari, Italy*
[e] *Joint Institute for Nuclear Research, Dubna, Russia*
[f] *Dipartimento di Energetica, Università di Firenze and INFN, Sezione di Bologna, Bologna, Italy*
[g] *Laboratori Nazionali di Frascati dell'INFN, Frascati, Italy*
[h] *Laboratori Nazionali di Legnaro dell'INFN, Legnaro, Italy*
[i] *Dipartimento di Fisica Nucleare e Teorica, Università di Pavia, and INFN Sezione di Pavia, Pavia, Italy*
[j] *Dipartimento di Fisica, Università di Torino and INFN, Sezione di Torino, Torino, Italy*
[k] *Politecnico di Torino and INFN, Sezione di Torino, Torino, Italy*
[ℓ] *Istituto di Fisica, Università di Trieste and INFN, Sezione di Trieste, Trieste, Italy*
[m] *Istituto di Fisica, Università di Udine and INFN, Sezione di Trieste, Trieste, Italy*

Received 18 December 1996; revised manuscript received 27 February 1997
Editor: L. Montanet

PII S0370-2693(97)00300-6

Abstract

The study of the $K^{\pm}K^{0}_{\rm miss}\pi^{\mp}\pi^{+}\pi^{-}$ channel (7016 events), from $\bar{p}p$ annihilations in a gaseous hydrogen target at NTP, with the OBELIX spectrometer at LEAR (CERN), is presented. A spin-parity analysis provides evidence for two axial vectors, one in the low $K\bar{K}\pi$ mass region, the well established $f_1(1285)$, decaying to $a_0(980)\pi$, the second, the 1^{++} component of the old puzzling E/ι, the $f_1(1420)$, decaying mainly to $K^*\bar{K}$, seen for the first time in $\bar{p}p$ annihilation at rest. The analysis confirms the dominant production of the pseudoscalar $\eta(1405)$, decaying mainly to $(K\pi)_S\bar{K}$, and the existence of a second pseudoscalar in the same mass region, the $\eta(1460)$, decaying mainly to $K^*\bar{K}$. © 1997 Published by Elsevier Science B.V.

1. Introduction

The search for non-$q\bar{q}$ mesons, states composed entirely of gluons (glueballs) or of a mixture of quarks, antiquarks and gluons (hybrids) or multiquarks states, has represented the main motivation of light meson spectroscopy over the last years. Since these objects are a direct prediction of Quantum ChromoDynamics (QCD), an experimental confirmation would be an important test of the theory and would give fundamental information on the behaviour of QCD in the confinement region. In addition, something has to be learned of the underlying spectrum of these states and in particular how they mix with standard $q\bar{q}$ states. Therefore, meson spectroscopy has become synonymous of *gluonium spectroscopy* and since the scientific case looks at the heart of confinement physics, an appropriate definition of this field of research is more properly *non-perturbative QCD* or *strong QCD*.

The beginning of gluonium spectroscopy can be dated with the discovery, in radiative J/Ψ decay [1,2], of a surprisingly large signal in the $K\bar{K}\pi$ effective mass spectrum. This signal was in the same mass region ($1400 \div 1500$ MeV) where a strong resonant peak had already been observed in $\bar{p}p$ annihilation at rest [3]. The controversial experimental evidence coming from the spectroscopy of this mass region created an intense debate, still not concluded, known as "E/ι puzzle", which can be stated as follows.

One, two, three or even more states, decaying to $K\bar{K}\pi$, $\eta\pi\pi$ or $\rho^0(770)\gamma$ have been observed in the "E/ι region" in a variety of different reactions and production mechanisms: there are experiments where only *one* resonance is observed with quantum numbers 0^{-+} (for instance, $\bar{p}p$ at rest in the $\eta\pi\pi$ mode [4]) or 1^{++} (for instance, central production [5]); or experiments where *two* pseudoscalars are observed (for instance, $\bar{p}p$ at rest looking for $K\bar{K}\pi$ decay [6]); or also experiments where *three* resonances are present (for instance, J/Ψ radiative decay [7,8]). The considerable uncertainty on the decay modes, especially concerning the $a_0\pi$ contribution to the $K\bar{K}\pi$ and $\eta\pi\pi$ final states, is another important element of the puzzle.

The interest to the case lies in the fact that some among those objects could be glueballs, hybrids, quasi-molecular or multiquark states. Concerning the two observed pseudoscalars (which are listed in the Review of Particle Physics under the unique $\eta(1440)$ [9]): the $\eta(1405)$, with dominant three-body decay $(K\pi)_S\bar{K}$ in the $K\bar{K}\pi$ mode, seen also in the $\eta\pi\pi$ final state, and the $\eta(1460)$ decaying only to $K^*\bar{K}$, and not seen in the $\eta\pi\pi$ mode, there are good arguments for considering one of them as an extra state not belonging to the 2^1S_0 nonet. The 1^{++} component of the E/ι, the isosinglet $f_1(1420)$, observed in the $K\bar{K}\pi$ final state and only weakly seen in the $\eta\pi\pi$ final state, can be considered as a good candidate for an extra state of the $^3P_1$ nonet.

For recent reviews on the E/ι case, and recent experimental results, see Refs. [10–14] and Refs. [15,16], respectively.

In this paper, the study of the $K^{\pm}K^{0}_{\rm miss}\pi^{\mp}\pi^{+}\pi^{-}$ channel, from $\bar{p}p$ annihilation in gaseous hydrogen at NTP, is reported. A spin-parity analysis was performed, according to which evidence was found for two axial vectors, one in the low $K\bar{K}\pi$ mass region, the well established $f_1(1285)$, decaying to $a_0(980)\pi$, the second being the isosinglet 1^{++} component of the old puzzling E/ι, the $f_1(1420)$, decaying mainly to

[1] On leave of absence from Joint Institute of Nuclear Research, Dubna, Moscow, Russia.

[2] On leave of absence from IFIN-HH, Bucharest, Romania.

$K^*\bar{K}$, seen for the first time in $\bar{p}p$ annihilation at rest. The analysis confirmed also the dominant production [6] of the pseudoscalar $\eta(1405)$, decaying mainly to $(K\pi)_S\bar{K}$, and the presence of a second pseudoscalar in the E/ι region, the $\eta(1460)$, decaying mainly to $K^*\bar{K}$ [6–8].

2. Data taking and event selection

The experiment was performed at the Low Energy Antiproton Ring (LEAR) of CERN, using the OBELIX spectrometer (whose detailed description can be found in Ref. [17]). OBELIX is a magnetic spectrometer consisting of four subdetectors: a Spiral Projection Chamber (SPC) as vertex detector, a Time-Of-Flight system (TOF) for trigger and TOF measurements, a Jet Drift Chamber (JDC) to determine momentum and energy loss (dE/dx) of charged particles, a High Angular Resolution Gamma Detector (HARGD) as electromagnetic calorimeter. The whole apparatus is immersed in a magnetic field, whose intensity reaches its maximum value of 0.5 T along its axis. Incoming antiprotons with a momentum of 105 MeV/c annihilated at rest in a gaseous hydrogen target at NTP. In investigating the $\bar{p}p \rightarrow K^{\pm}K^0_{\rm miss}\pi^{\mp}\pi^+\pi^-$ channel, only the information coming from TOF and JDC was used in the analysis.

About 24 million 4-prong events were collected in 18 days. A trigger requiring 4 hits in the inner TOF barrel, 3–4 hits in the outer barrel and at least one track with TOF $\geq$ 8.5 ns was employed [18], in order to select final states with at least one charged kaon. The enrichment factor provided by this trigger, with respect to minimum bias events, was 5.

The data selection procedure was the same as in Refs. [6,19]. The analysis program selected all events with 4 reconstructed charged tracks in the JDC and null total charge. Quality cuts, consisting in selecting events having good χ^2/track(< 1.5 for track length less than 30 cm, < 3 for other tracks), vertex accuracy better than 1 cm and momentum resolution $\Delta p/p \leq 10\%$, were applied. Events having one or more tracks with a vertex impact parameter greater than 3 cm, were rejected. Details on the apparatus acceptance have been given in a previous work [6].

The K^0 was not detected but reconstructed by 1C kinematical fit. The selection criteria were based

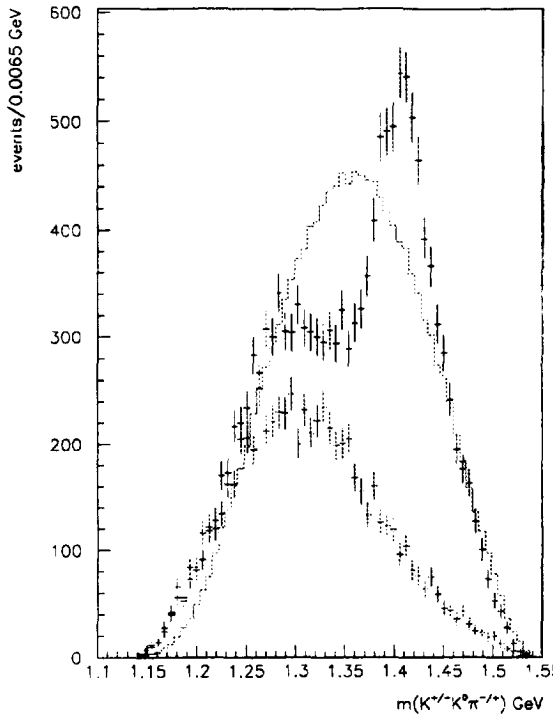

Fig. 1. The experimental and phase space (histogram) double-entry invariant mass distributions of the neutral $K\bar{K}\pi$ system and the double charge $K^{\pm}K^0\pi^{\pm}$ mass distribution.

mainly on the identification of the charged kaon by dE/dx. Particle identification was applied to all particles detected in the final state by requiring the presence of one particle with energy loss in the kaon region ($p_K \leq 400$ MeV/c) and two other particles, with opposite charge to the kaon, with energy loss in the pion region.

Channels like:

- $\pi^+\pi^-\pi^+\pi^-(n\pi^0)$ $[n = 0, 1]$
- $K^+K^-\pi^+\pi^-$
- $K^{\pm}K^0_s\pi^{\mp}(n\pi^0)$ $[n = 0, 1]$ $(K^0_s \rightarrow \pi^+\pi^-)$

were rejected by kinematical fit and did not contribute to the K^0 missing mass region.

The square missing mass distribution of the $K^{\pm}\pi^{\mp}\pi^-\pi^-$ selected events shows a clear evidence of a K^0 signal. Under the K^0 peak it is present a residual contamination ($25 \pm 5\%$) of events coming, above all, from the $\pi^+\pi^-\pi^+\pi^-n\pi^0$ ($n > 1$) channel, with one pion misidentified as a kaon, and from the $K^+K^-\pi^+\pi^-\pi^0$ final state, with one kaon decaying close to the vertex region. Such background

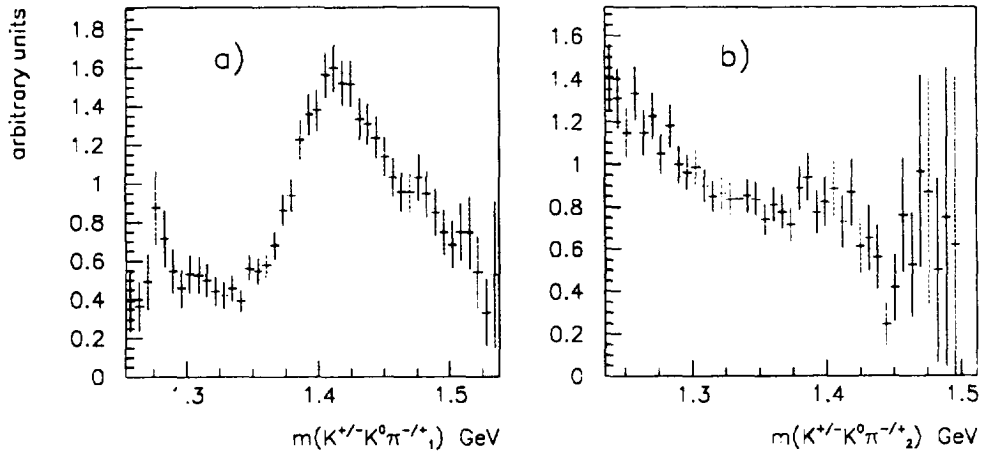

Fig. 2. The divided-mass-distributions for the: a) $(K\bar{K}\pi_1)$ and, b) $(K\bar{K}\pi_2)$ combinations.

has been extensively studied using Monte Carlo simulations and experimental data. The contamination, which comes mostly from the second channel listed above, has a distribution which turns out similar to the phase space distribution, as observed also in our previous work [6]. The final number of events in the missing mass interval $0.21 < M^2 < 0.31$ GeV^2, selected for the spin-parity analysis, was 7016.

3. The $K\bar{K}\pi$ mass distributions

Fig. 1 shows the experimental and phase space double-entry mass distributions of the $K^{\pm}K^0_{\rm miss}\pi^{\mp}$ system, together with the double charge $K^{\pm}K^0\pi^{\pm}$ mass spectrum. A prominent signal in the mass region around 1410 MeV is evident, with a strong departure from the phase space distribution.

Due to the presence of two identical pions in the annihilation final state, the scatter plot $K\bar{K}\pi_1$ vs $K\bar{K}\pi_2$ must be symmetrical and can be folded with respect to the diagonal (by ordering, for example, the identical pions such that $m(K\bar{K}\pi_1) > m(K\bar{K}\pi_2)$). This way, the two single-entry mass distributions (folded scatter plot projections) have very different features. The $K\bar{K}\pi_1$ invariant mass distribution shows a clear signal around 1410 MeV, and an enhancement around 1280 MeV (which was not apparent in the double-entry plot). The $K\bar{K}\pi_2$ spectrum peaks around 1300 MeV and looks very much alike the double-charge mass distribution, without signs of resonant activity.

In order to emphasize resonant signals, the neutral $K\bar{K}\pi_1$ and $K\bar{K}\pi_2$ mass distributions were divided by the equivalent Monte Carlo phase space (which takes into account the apparatus acceptance). Both a narrow ($\Gamma \cong 30$ MeV) signal around 1280 MeV and a wider and asymmetric peak around 1420 MeV can be observed in the $K\bar{K}\pi_1$ divided-mass-distribution (Fig. 2a). The $K\bar{K}\pi_2$ divided-mass-distribution (Fig. 2b) does not show, on the contrary, any resonant structure. The asymmetrical structure of the peak around 1420 MeV in Fig. 2a suggests the presence of more than one resonance in the 1380 ÷ 1520 MeV mass interval.

Indeed, in the sample of selected events, the level of contamination background (expected to be around 25% and proved to have a distribution similar to the phase space), decreases down to 14% when $M(K\bar{K}\pi_2) < 1260$ MeV, and it is only at the level of 8–9% in the E/ι mass region ($M(K\bar{K}\pi_1) > 1360$ MeV). The $K\bar{K}\pi_1$ invariant mass distribution for such a reduced sample of events (1891 events) is shown in Fig. 3, together with the contaminating background spectrum. The mass bin width of this distribution was set equal to the experimental $K\bar{K}\pi$ mass resolution (6.5 MeV in the E/ι region). This single-entry spectrum, free from the combinatorial background and with a reduced contamination level, shows, in addition to the signal at 1280 MeV, hints for three sub-structures in the region between 1400 and 1500 MeV.

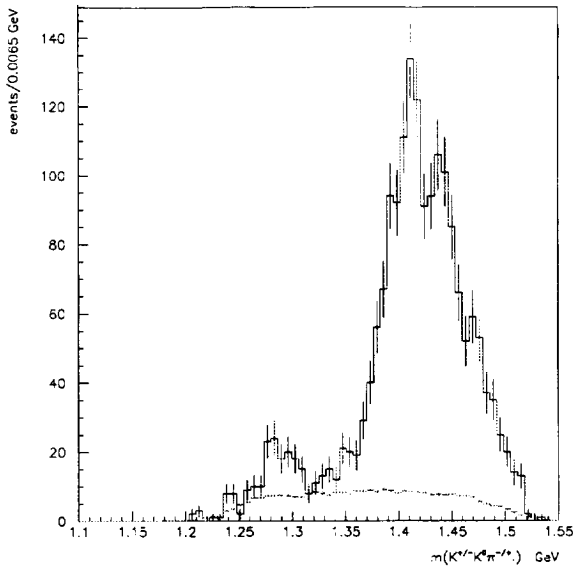

Fig. 3. The $K\bar{K}\pi_1$ mass spectrum for $M(K\bar{K}\pi_2) < 1260$ MeV, together with the contaminating background.

4. Amplitude construction for the $\bar{p}p \to K^{\pm}K^{0}_{\mathrm{miss}}\pi^{\mp}\pi^{+}\pi^{-}$ channel

For the spin-parity analysis, the five-body final state was considered as a chain of two-body intermediate states, according to the prescription of the isobar model.

$$\bar{p}p \longrightarrow \underset{(K\bar{K}\pi)}{A} + \underset{(\pi\pi)}{B}$$

$$\searrow$$

$$a + b$$

$$\swarrow \qquad \searrow$$

$$\pi,\ K$$

$$(K\pi)_{I=1} \equiv K^{*}(892)$$
$$(K\bar{K})_{I=0} \equiv a_0(980)$$
$$(K\pi)_{I=0}$$

The total amplitude, symmetrized for two identical pions, was constructed by summing all the elementary amplitudes over all possible $\bar{p}p$ J^{PC} states ($J = 0, 1$; $P = \pm$; $C = +$):

$$|M(y)|^2 = \sum_{J^{PC}} |A_{J^{PC}}(y)|^2, \tag{1}$$

Here y is a point in the 8-dimensional phase space of the 5-body final state and

$$A_{J^{PC}}(y) = \sum_k x_k e^{i\phi_k} A_k(y), \tag{2}$$

where A_k are the elementary amplitudes, with x and ϕ free parameters.

The elementary amplitudes for the $\bar{p}p \to E/\iota\,\pi\pi$ process were the following:

(1) $E/\iota \to K^{*}\bar{K}$

$$A_k = A(\pi\pi)BW(E/\iota)[BW(K^{*\pm})D(K^{*\pm}) + G \cdot BW(K^{*0})D(K^{*0})], \tag{3}$$

in which G is the E/ι G-parity and D represents the angular component of the amplitude written according to the Zemach tensor formalism. For the energy part of the amplitude a standard relativistic Breit-Wigner form ($\sim 1/(s - m^2 + i \cdot m \cdot \Gamma)$, with a constant width, and centrifugal barrier factors ($\sim q^l$) included in the Zemach tensors, were used.

(2) $E/\iota \to (K\bar{K})_S\pi$

$$A_k = A(\pi\pi)BW(E/\iota)S_0(K\bar{K})D(K\bar{K}), \tag{4}$$

in which the scalar $K\bar{K}$ threshold enhancement (the $a_0(980)$) is described by a coupled-channel Flattè function [20] ($S_0(K\bar{K})$), with parameters taken from a recent work [21].

(3) $E/\iota \to (K\pi)_S\bar{K}$

$$A_k = A(\pi\pi)BW(E/\iota)[S_0(K^{\pm}\pi^{\mp})D(K^{\pm}\pi^{\mp}) + G \cdot S_0(K^{0}\pi^{\mp})D(K^{0}\pi^{\mp}), \tag{5}$$

where $(K\pi)_S$ - the $(K\pi)$ S-wave interaction used to describe the E/ι direct three-body decay - is also parameterized by a scattering length function [22].

The neutral dipion, recoiling against the $K\bar{K}\pi$ isobar, has a mass spectrum which does not follow a phase space like distribution. Since the dipion invariant mass does not exceed 500 MeV, it is reasonable to assume that the isoscalar $\pi\pi$ interaction takes place mainly with relative orbital angular momentum $l = 0$. The corresponding term in the amplitude was constructed from a parameterization of existing data from literature [23] using a scattering length function.

The reaction channels taken into consideration were:

(1) $\bar{p}p \to X\pi\pi$, where X is a 1^{++} or a 0^{--} resonance;

(2) $\bar{p}p \rightarrow f_1(1285)\pi\pi$, with resonance parameters taken from the Review of Particle Physics [24];
(3) $\bar{p}p \rightarrow K^*\bar{K}\pi\pi$, $a_0\pi\pi\pi$, $(K\pi)_S\bar{K}\pi\pi$, to account for direct production of $K^*(892)$, $a_0(980)$ and direct annihilation into a non-resonant final state, respectively;
(4) background contamination from other final states as an incoherent constant phase space like term.

Following the P (or Q) matrix formalism [25] for resonance production, the relative phase between different decay channels of the same resonance were fixed to the same value.

Data were fitted by minimizing the likelihood function event by event:

$$\mathcal{L} = -2\log(L) = -2\sum_{i=1}^{N}\log\left[(1-f)\frac{|M(y_i)|^2}{\int|M(y)|^2dy}+f\right], \quad (6)$$

where N is the total number of events and f describes an incoherent phase space like background contribution. Masses and widths of E/ι resonances were free parameters. The analysis was performed assuming dominance of the lowest possible values of relative angular momenta [6,26]. This hypothesis, motivated by the kinematics of the annihilation at rest, leads to production of 0^{-+} and 1^{++} ($K\bar{K}\pi$) states from initial $^1S_0$ and $^3P_1$ protonium waves, respectively. Once the best fit solution was found, several tests were performed in order to establish the goodness of the above assumption.

5. Spin parity analysis

5.1. Global fit

The strategy followed in a global fit is to look for the minimum set of amplitudes which provides the best representation of the data without redundancy in the number of fitting parameters. The maximum likelihood method was adopted to estimate the goodness of the fit, although, for the hypothesis test, the sum of χ^2 (obtained by comparing various experimental distributions with the predicted ones) for the most relevant distributions, was used.

The first and simplest fitting hypothesis was to assume the presence of a single resonance in the region around 1410 MeV of the neutral $K\bar{K}\pi$ system, with a spin-parity assignment of a pseudoscalar or an axial vector. Concerning the resonance decays, the intermediate states $a_0\pi$, K^*K and the direct decay $(K\pi)_S\bar{K}$ were considered simultaneously. A total of 8 free parameters were used to construct the amplitude. A similar approach was followed in the analysis of the same final state selected from a data sample in which the antiproton annihilations took place in a liquid hydrogen target in the OBELIX spectrometer [6].

Just as in that analysis, the quality of the fit was poor, independently of the resonance spin-parity assignment. Nevertheless, a comparison between the two hypotheses, namely $J^{PC} = 0^{-+}$ or 1^{++}, showed clearly that the main resonant contribution to the neutral $K\bar{K}\pi$ system was due to a 0^{-+} state. The result of the one-resonance fit indicated also a dominance of the direct decay compared to the $a_0\pi$ and $K^*\bar{K}$ modes, in agreement with the previous results.

The large value of χ^2 (560 for 383 data points), calculated on various invariant mass distributions, a fraction of incoherent background above the expected value, and the predicted mass spectrum which fitted poorly the asymmetric $K\bar{K}\pi$ lineshape above 1400 MeV, suggested altogether the need for a more complex structure of the fitting amplitude.

Indeed, the conclusion of the results from the previous work on liquid hydrogen, which demonstrated the existence of two nearby pseudoscalar states, together with the present experimental conditions (gaseous hydrogen provides higher angular momenta in the initial state, which might excite resonances with different quantum numbers) and the indications provided by the experimental mass distribution (see, for example, Fig. 3), justified the hypothesis of an increasing of the number of resonances from two to three in the E/ι mass region. A partial wave analysis (PWA) of the considered final state was then performed.

5.2. Partial wave analysis

In order to perform a PWA of the selected reaction, the problem of having two identical pions contributing to the neutral $K\bar{K}\pi$ system had first to be addressed. The solution, described in Section 3, consisted in selecting the region of available phase space

in which only one of the two combinations ($K\bar{K}\pi_1$: here called the "active" combination) had the largest resonant contribution, the other one ($K\bar{K}\pi_2$: the "passive" combination) being mostly phase space like. In this kinematical region a PWA of only the "active" $K\bar{K}\pi$ combination was applied, without loosing the relevant physics information. This assumption was tested by applying a global fit to the experimental data within the selected region, with and without the symmetrization of the best fitting amplitudes with respect to the two identical pions. The minimization procedure yielded basically the same likelihood value in the two cases.

The PWA was performed on the $K\bar{K}\pi_1$ mass region from 1360 to 1510 MeV, in adjacent bins of 30 MeV, with the requirement $M(K\bar{K}\pi_2) < 1300$ MeV. The change in the cut value from 1260 to 1300 MeV, to increase statistics, produced no practical effect on the results of the analysis. The number of selected events was 2950. In order to check the stability of the fit, as well as of the general pattern of the intensity spectra and the relative phase motions, the analysis was repeated using different bin positions and sizes.

An extensive iterative fitting procedure with different spin-parity hypotheses and different initial values of the amplitude parameters showed that the most significant contributions to the final state comes from both resonant pseudoscalar and axial vector states. The partial amplitudes considered in this analysis were those which described the (0^{-+}) and (1^{++}) $K\bar{K}\pi$ isobar decay into $K^*\bar{K}$ + c.c., $a_0\pi$, as well as into $(K\pi)_S\bar{K}$ + c.c.

In more detail, the results of the PWA were:

1) The (0^{-+}) $a_0\pi$ and $(K\pi)_S\bar{K}$ intensity spectra associated to annihilations from protonium $^1S_0$ state showed a clear enhancement at M = 1410 MeV (Fig. 4). The two signals can be ascribed to the same resonance. Indeed, a fit of the two peaks with relativistic Breit-Wigner functions yielded similar values for mass and width, namely: M = 1420± 10 MeV and Γ = 38 ± 5 MeV. The 0^{-+} ($K^*\bar{K}$) S-wave intensity spectrum showed also activity near 1400 MeV.

Since the phase motions (not shown) of the $(0^{-+})a_0\pi$ and the $0^{-+}(K^*\bar{K})$ partial waves, with respect to the phase of the $(0^{-+})(K\pi)_S\bar{K}$ wave in the region 1360 ÷ 1440 MeV were almost constant, then, most likely, all three 0^{-+} partial waves considered in the present analysis resonate together at a mass value near 1420 MeV.

2) The (0^{-+}) $K^*\bar{K}$ S-wave intensity spectrum showed, besides the activity near 1400 MeV, a peak at 1460 MeV (Fig. 4).

A fit of that high mass peak with a relativistic Breit-Wigner function yielded a value of the mass equal to 1462 ± 5 MeV. The phase of this partial amplitude relative to the $(0^{-+})(K\pi)_S\bar{K}$ wave showed a rapid forward motion (Fig. 4), which confirmed the presence of a resonant 0^{-+} state at 1460 MeV in agreement with the results in liquid hydrogen [6].

3) The (1^{++}) $K^*\bar{K}$ partial wave intensity, associated to annihilations from the $^3P_1$ protonium state, showed a clear enhancement around 1430 MeV (Fig. 4). The Breit-Wigner fit to this distribution yielded $M = 1427 \pm 4$ MeV and $\Gamma = 51 \pm 10$ MeV. This peak can be identified with the $f_1(1420)$ observed in J/Ψ radiative decay, central production, $\gamma\gamma$ collisions, peripheral production. The $(1^{++})(K\pi)_S\bar{K}$ partial wave, on the contrary, provided a negligible contribution to the annihilation from P-wave. Because of the small contribution of other (1^{++}) partial waves, the relative phase motion of the $(1^{++})K^*\bar{K}$ wave could not be unambiguously determined.

5.3. Global best fits

5.3.1. Low background data sample

In order to confirm the existence of the axial vector $f_1(1420)$, as well as to establish the significance of the second pseudoscalar $\eta(1460)$, a global fit to a selected sample of 2950 events, with $M(K\bar{K}\pi_2) < 1300$ MeV and $M(K\bar{K}\pi_1)$ between 1360 and 1510 MeV (as in the PWA), was performed. In this region of phase space the background contribution was estimated via MC simulations to be of the order of 8–9%.

Three resonant states: two 0^{-+} and one 1^{++} were introduced in the total amplitude. The two pseudoscalar states, coming from the same initial state ($^1S_0$), were added coherently. This way, the amplitude was constructed with 7 free parameters. The fits were repeated for various fixed resonance masses and widths. The minimization of the likelihood was obtained for the following mass and width values:

$\eta(1405)$: M = 1406 MeV, Γ = 48 MeV

$\eta(1460)$: M = 1465 MeV, Γ = 100 MeV

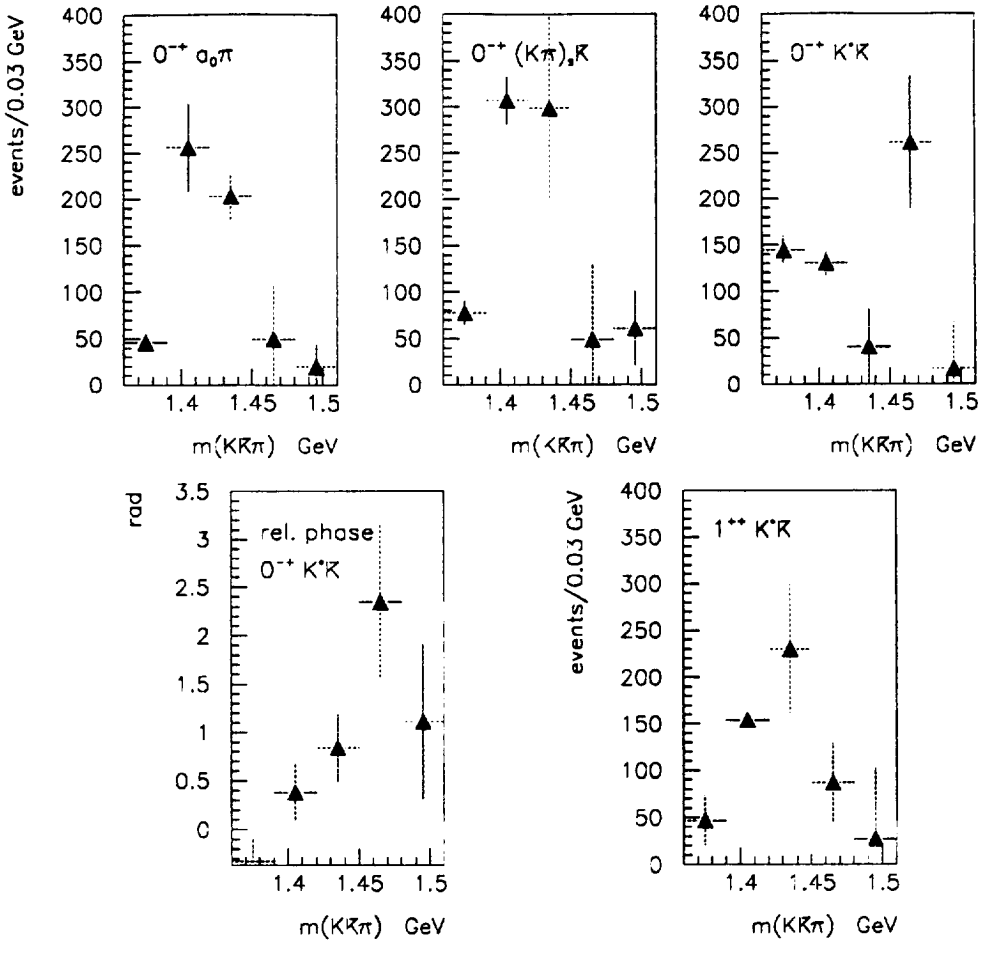

Fig. 4. Partial wave analysis: partial wave intensities and the $(0^{-+})K^*\bar{K}$ S-wave phase motion.

$f_1(1420)$: M = 1425 MeV, Γ = 42 MeV

This form of the amplitude provided an excellent description of the data in the considered kinematical domain. The results of the global fit on the low background data sample confirmed the significance of the axial vector resonance, as well as the presence of a second pseudoscalar state.

Inverting the spin-parity of the $f_1(1420)$ and of the $\eta(1460)$ in the best fit solution provided worse results ($\Delta\mathcal{L} = 26$).

5.3.2. Low $K\bar{K}\pi$ mass region

An independent fit of the data in the low $K\bar{K}\pi$ invariant mass region ($M(K\bar{K}\pi) < 1400$ MeV) was performed in order to establish the nature of the signal around 1280 MeV. The total number of fitted events was 2616.

Due to the presence of strong tails from the nearby resonances, the relative decay fractions of $\eta(1405)$ were fixed in the fit, the only free parameters in the amplitude being those which described contributions from both the axial vector $f_1(1285)$ and the pseudoscalar $\eta(1295)$, from initial S- and P-waves. For the decay of the two resonances only the $a_0\pi$ mode was considered (indeed the $f_1(1285)$ and the $\eta(1295)$ decays are mainly through $a_0\pi$ [21,27]). The limited statistics prevented from investigating additional decay modes. Mass and width of $f_1(1285)$ and $\eta(1295)$ were fixed to the nominal values.

Table 1
Relative contributions (in percent) from spin-parity analysis of the low $K\bar{K}\pi$ mass region: in the first and second row, respectively, the results with and without $f_1(1285)$ and $\eta(1295)$, together with the S-and P-wave and background contributions are presented. $\mathcal{L}$ is the maximum likelihood function, $N_p = 293$.

$\mathcal{L}$	χ^2/N_p	$\eta(1295)$	$f_1(1285)$	S	P	Bkg.
−1607	1.26	0.1±0.1	4.0±1.0	61.4±2.5	13.3±2.5	25.3±3.5
−1538	1.67	-	-	52.3±2.5	10.3±2.5	37.4±3.9

The fits were repeated on a sub-sample of 1543 events satisfying the requirements $M(K\bar{K}) < 1060$ MeV, to increase the sensitivity to the $a_0(980)$.

The fit results for the 2616 events are summarized in Table 1 and are shown, superimposed to the experimental distributions, in Fig. 5. The production of the $f_1(1285)$ turned out at the level of a few percent, whereas the $\eta(1295)$ seemed absent in the data.

5.3.3. Full data sample

In the final step of the analysis a global fit of the full data sample (7016 events) was performed. The total amplitude accounted for: production of three resonances in the region around 1420 MeV, decaying to unstable intermediate states ($a_0\pi$ and $K^*\bar{K}$) and directly into $K\bar{K}\pi$; a 1^{++} state at 1285 MeV decaying to $a_0\pi$; direct contributions of a_0, K^* and direct 5-body annihilation from initial $^1S_0$ and $^3P_1$ protonium waves; a background term. In order to determine the resonance parameters, besides an intensive grid search, mass and width were allowed to be free in the global fit.

The best fit, with only 9 free parameters (unaccounting for variable masses and widths), was obtained when the S-wave was saturated by the production of two pseudoscalars and the P-wave was saturated by the two axial vectors $f_1(1285)$ and $f_1(1420)$, plus direct production of K^*.

The importance of the direct production terms is better emphasized by the inspection of some angular distributions. The angular distribution of one kaon from the $K\bar{K}\pi$ system recoiling against the spectator dipion, as well as the angular distribution of one pion in the rest frame of the two identical pions, are sensitive to the direct production terms in the amplitude and are best fitted when a direct production of $K^*(892)$ is taken into account in the amplitude.

The best fit solution provided small values for the relative phases of the P-wave elementary amplitudes: $\phi = -0.23 \pm 0.19$ rad for K^* direct production and $\phi = -0.09 \pm 0.1$ rad for $f_1(1420)$.

Moreover, when direct K^* production was not considered, and therefore P-wave was saturated by the two axial vectors, the relative phase of the $f_1(1420)$ changed to $\phi = -1.74 \pm 0.22$ rad. And, analogously, by excluding the $f_1(1420)$, the relative phase of K^* production became $\phi = 0.79 \pm 0.23$ rad. In both cases the phases were far from the expected values of 0 or π [28]. Similarly, the relative phase of the two pseudoscalars was found to be close to zero.

The results of the best fit obtained in the hypothesis of two pseudoscalars and one axial vector in the E/ι region, plus the 1^{++} $f_1(1285)$ and direct K^* production, are reported in Table 2, first line. The first pseudoscalar, the $\eta(1405)$, is the dominant contribution and it has mainly a three-body decay. The existence of a second pseudoscalar, seen for the first time in $\bar{p}p$ annihilation at rest in liquid hydrogen by OBELIX [6], is confirmed, with a main $K^*\bar{K}$ decay mode. Mass, width and decay modes of the two pseudoscalars are in agreement with the values obtained from the analysis of the liquid hydrogen data sample.

A quantitative evidence of the two axial vectors $f_1(1285)$ and $f_1(1420)$ represents a significant result of the fit. The ratio of their fractional contribution (~ 1.5) is in agreement with the value obtained from central production data. Besides, looking for a possible $a_0\pi$ decay mode of the $f_1(1420)$, an upper limit of 1% was found. This percentage is in agreement with the ratio $\mathrm{Br}(f_1(1420) \to a_0\pi)/(f_1(1285) \to a_0\pi) = 0.2 \pm 0.1$ obtained by GAMS [27] in the analysis of the E/ι decay to $\eta\pi^0\pi^0$.

The background contribution resulting from the best fit ($\sim 21\%$) is consistent with the experimental value.

In order to test the J^{PC} assignment of the structure at 1420 MeV, a fit with a pseudoscalar replacing the $f_1(1420)$, but maintaining the other features of the amplitude, was performed. A normalized χ^2 of 1.33 for the $K\bar{K}\pi$ mass distribution and a change in the likelihood value by $\Delta\mathcal{L} = 37$ demonstrated the axial vector nature of the structure at 1420 MeV.

In the second line of Table 2 a check of the fit sensitivity to the presence of the $f_1(1420)$ in the data sample is reported. Removing the $f_1(1420)$ causes a worsening of the fit in terms of χ^2 and likelihood

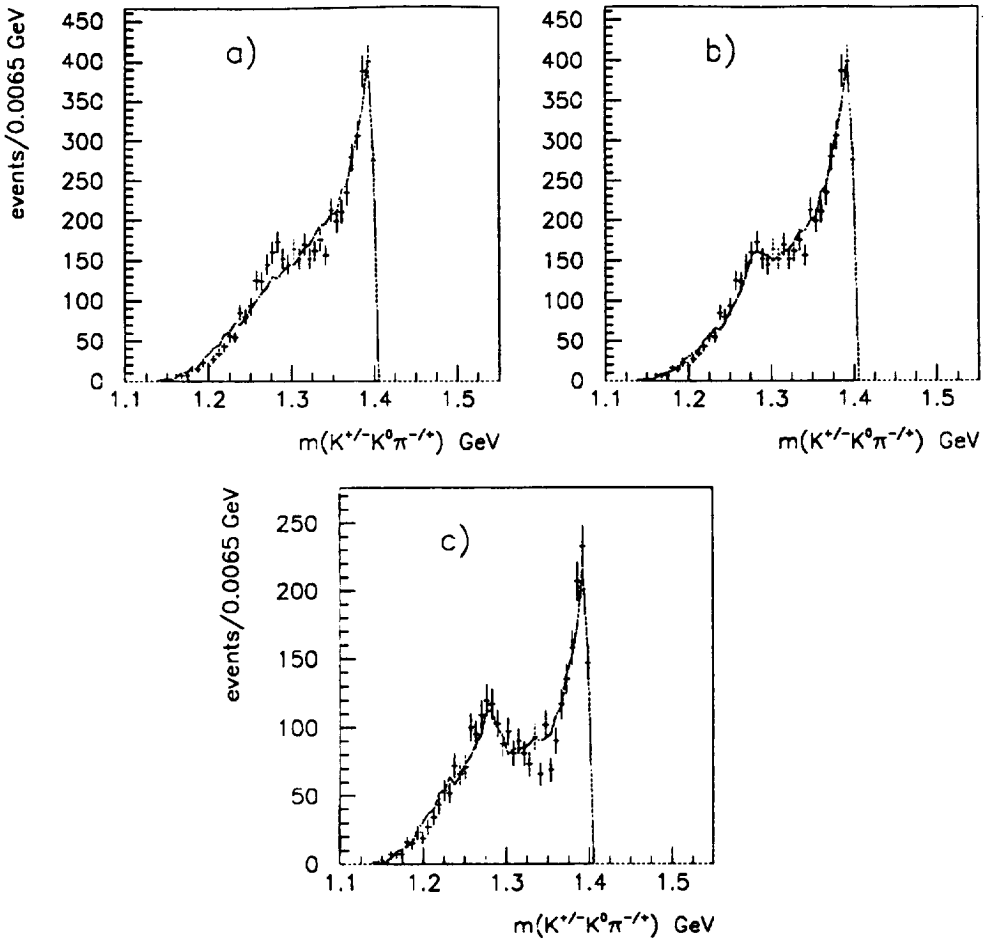

Fig. 5. $K\bar{K}\pi$ mass distribution in the region of $f_1(1285)$: a) fit without the $f_1(1285)$, b) fit with the $f_1(1285)$ and c) fit with $f_1(1285)$ and selected $K\bar{K}$ in the $a_0(980)$ mass region.

Table 2
Relative contributions (in percent) from spin-parity analysis of the low $K\bar{K}\pi$ mass region: in the first and second row, respectively, the results with and without $f_1(1285)$ and $\eta(1295)$, together with the S-and P-wave and background contributions are presented. $\mathcal{L}$ is the maximum likelihood function, $N_p = 293$.

$\eta(1405)$			$\eta(1460)$	$f_1(1285)$	$f_1(1420)$	dir. prod.	Bkg.	$\mathcal{L}$	χ^2/N_1	χ^2/N_2
$a_0\pi$	$K^*\bar{K}$	$(K\pi)_S\bar{K}$	$K^*\bar{K}$	$a_0\pi$	$K^*\bar{K}$	$K^*\bar{K}\pi\pi$				
9.3 ± 0.9	6.5 ± 0.5	41.3 ± 1.2	5.4 ± 0.7	3.4 ± 0.5	5.2 ± 1.1	8.2 ± 1.5	20.7 ± 1.5	−6027	1.23	0.97
	mass = 1407 ± 1		1459 ± 3		1422 ± 4					
	width = 48 ± 1		108 ± 5		42 ± 9					
9.7 ± 0.7	6.0 ± 0.4	42.0 ± 1.5	5.5 ± 0.9	3.5 ± 0.5		11.7 ± 1.6	21.6 ± 1.3	−6011	1.30	1.31
	mass = 1413 ± 1.		1458 ± 3							
	width = 51 ± 1.		113 ± 5							

($\Delta\mathcal{L} = 16$), the latter being larger than the statistical fluctuation of the likelihood function ($\Delta\mathcal{L} \approx 2$), as obtained from a Monte Carlo simulation.

When one removes the P-wave $K^*\bar{K}$ direct production, the width of the $f_1(1420)$ increases ($\Gamma \approx 92$ MeV), as well as its mass, both to values in disagreement with those quoted in the Review of Particle Physics. The quality of the fit remains, however, satisfactory.

The hypothesis of dominance of relative angular momentum $l = 0$ between the $K\bar{K}\pi$ resonance and the dipion, was tested against possible contributions from partial waves leading to relative $l = 1$. In the analysis of the liquid hydrogen data [6], possible contributions from initial $^1S_0$ wave to the production of $f_1(1420)$ had been already excluded. In this analysis, two independent fits, removing $f_1(1420)$ and allowing for production of $\eta(1405)$ and $\eta(1460)$ from initial $^3P_1$ wave, respectively, yielded worse results, and excluded the possibility that higher order contributions from the pseudoscalars could simulate the axial signal.

A systematical uncertainty (of the order of 2–3 times the statistical errors) in the values of mass and width of resonances turns out from small variations of the amplitude. A realistic estimate of the resonance parameters was obtained by taking them into account. They are:

$\eta(1405)$: $M = 1407 \pm 5$ MeV, $\Gamma = 48 \pm 5$ MeV

$\eta(1460)$: $M = 1464 \pm 10$ MeV, $\Gamma = 105 \pm 15$ MeV

$f_1(1420)$: $M = 1425 \pm 8$ MeV, $\Gamma = 45 \pm 10$ MeV

The mass and the width of the $f_1(1420)$ is in good agreement with the world average values given by the Review of Particle Physics.

The results of the best fit are shown in Fig. 6 superimposed to some experimental mass distributions.

6. Conclusions

To summarize the results of the global fits and of the partial wave analysis of an overall sample of 7016 $p\bar{p}$ annihilations in gaseous hydrogen at NTP into the final state $K^{\pm}K^0_{\rm miss}\pi^{\mp}\pi^+\pi^-$, evidence was found for two pseudoscalars and one axial vector in the E/ι mass region ($1400 \div 1500$ MeV), which can be identified with the $\eta(1405)$, $\eta(1460)$ and $f_1(1420)$, respectively. Moreover, evidence for the $f_1(1285)$ was also found, in agreement with previous observation [26]. Specifically:

(1) The two axial vectors are seen together for the first time in $\bar{p}p$ annihilation at rest.

The presence of the $f_1(1285)$ in the data was required by all fitting hypotheses, and its contribution remained stable at the level of 3–4%. The $f_1(1285)$, always seen together with the $f_1(1420)$ in all experiments which observed only the axial vector in the E/ι region, is now seen for the first time together with the pattern of the two pseudoscalars and the axial vector, a feature not evident in J/Ψ decay measurements.

Many indications point to the existence of the $f_1(1420)$:

(a) in a PWA, the (1^{++}) $K^*\bar{K}$ partial wave intensity associated to annihilations from the $^3P_1$ protonium state, shows a clear enhancement around 1430 MeV. The Breit-Wigner fit to this distribution yields $M = 1427 \pm 4$ MeV and $\Gamma = 51 \pm 10$ MeV;

(b) the results of the various global fits and of the partial wave analysis provide mass, width and decay modes in very good agreement with the world average values quoted for the $f_1(1420)$ in the Review of Particle Physics.

(c) the production ratio with the $f_1(1285)$ has the same value as measured in the experiments which observed the production of both resonances;

(d) the exclusion in the P-wave of an axial vector around 1420 MeV worsens both the likelihood value beyond the statistical uncertainty, and the χ^2 of the $K\bar{K}\pi$ mass distribution;

(e) moreover, by excluding the $f_1(1420)$ in the fit, the relative phase of the elementary amplitude for K^* direct production changes from a value near zero, found in the best solution, to the value $\phi = 0.79 \pm 0.23$ rad;

(2) The first pseudoscalar, $\eta(1405)$, is by far the dominant contribution, it is very stable against modifications of the amplitude and it has mainly a three-body decay, with additional small equal fractions of $a_0\pi$ and $K^*\bar{K}$ decay. The relative

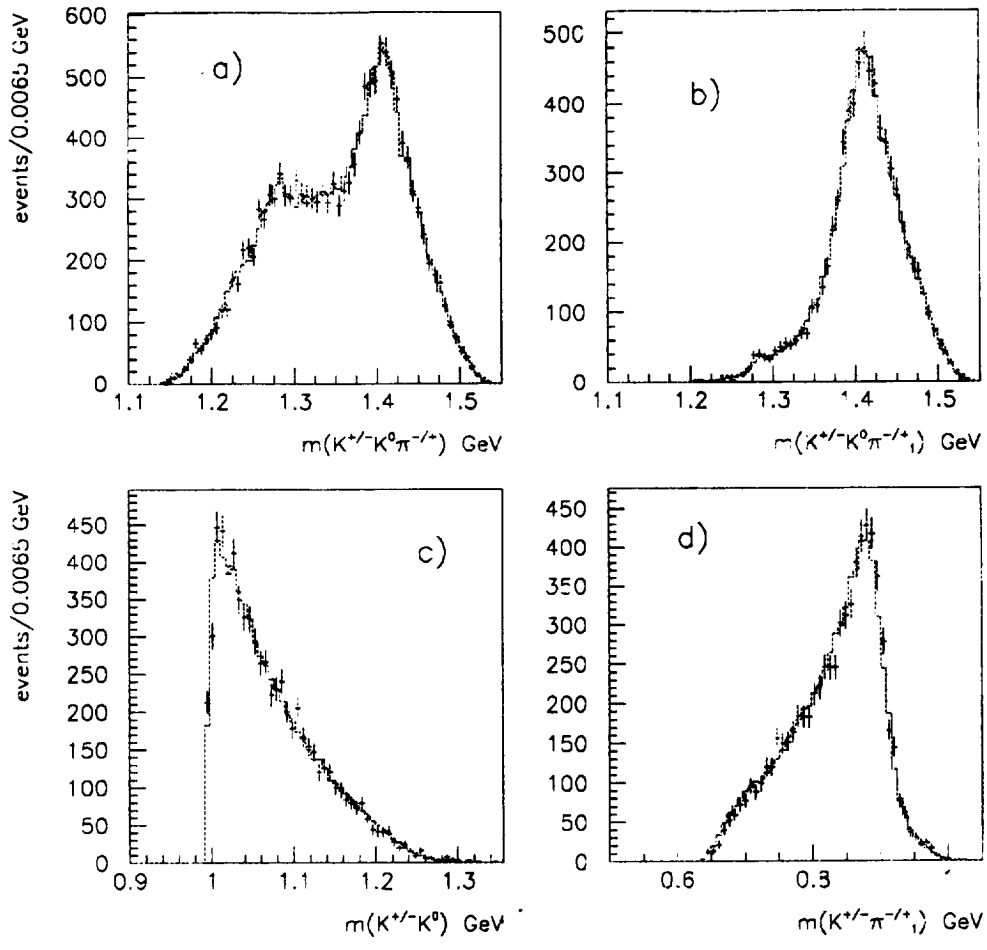

Fig. 6. Results of the spin-parity best fit: $(K\bar{K}\pi)$ invariant mass spectrum for a) two-entries and b) one-entry $(K\bar{K}\pi_1)$; c) $K\bar{K}$ invariant mass and d) neutral $(K\pi)$ spectrum.

weights of $\eta(1405)$ decays into $(K\pi)_S\bar{K}$, $a_0\pi$, $K^*\bar{K}$ are 6 : 1.5 : 1. Mass and width are M = 1407 ±5 MeV, Γ = 48 ± 5 MeV. These results confirm the previous ones obtained from $\bar{p}p$ annihilation in liquid hydrogen [6].

(3) The existence of a second pseudoscalar, seen for the first time in $\bar{p}p$ annihilation at rest in liquid hydrogen [6], is unambiguously confirmed. The direct production from S-wave of other intermediate states cannot entirely simulate the second pseudoscalar, even if its contribution gets slightly decreased compared to the previous result. The dominant decay mode is confirmed to be $K^*\bar{K}$. Mass and width are M = 1464 ± 10 MeV, Γ = 105 ± 15 MeV.

(4) There is no indication in these data of the presence of the pseudoscalar $\eta(1295)$. The same negative result was obtained from the liquid hydrogen data [6], where pseudoscalar production should be favoured, in principle, due to the protonium S-wave annihilation dominance.

QCD sum rules predict [29] the mass of the lighter pseudoscalar glueball to be in the range 1400 ÷ 1600 MeV. Lattice QCD calculations give a much higher value for such mass [30,31]. Arguments in favour of a glueball interpretation of one of the two resonances under the $\eta(1440)$ were proposed. A recent analysis [32] of the structure of the $\eta(1440)$, performed

using a mixing model with non-strange, strange and glueball basic states, shows that the $\eta(1405)$ can be a dominant pseudoscalar glueball. The sizeable direct three-body decay, confirmed also in the $\eta\pi\pi$ decay mode [4,27] might add support to the glueball interpretation. Another hypothesis was proposed for the lighter 0^{-+}: to be a hybrid state [33], made by coupling a $q\bar{q}$ state with a transverse electric gluon. Such a state, predicted [34] around 1400 MeV, is expected to decay via $a_0(980)\pi$ and $\eta(\pi\pi)_S$.

Concerning the $f_1(1420)$, it is one of the most interesting objects from the point of view of the existence of non-$q\bar{q}$ states. Until recently, it has been considered the $s\bar{s}$ member of the 1^{++} nonet. However, this interpretation is in contradiction with several experimental results [35–38]. Therefore, three possibilities are left: either the $f_1(1420)$ belongs to the 1^{++} excited nonet, but with a mixing angle far from the ideal one, or it is a real exotic state or, in the third case, it is a cusp effect due to the opening of the $K^*\bar{K}$ threshold. A glueball hypothesis can be ruled out [39], as well as a 4-quark state [39]. The hypothesis of a hybrid [40] seems not to be incompatible with the data. More probably, the $f_1(1420)$ is a molecule: either a $K^*\bar{K}$ molecule, of the type supported by Weinstein and Isgur [41], or of the type suggested by Longacre [42], in which a pion orbits in a P-wave around a $(K\bar{K})_S$ system.

References

[1] D.L. Scharre et al., Phys Lett. B 97 (1980) 329.
[2] C. Edwards et al., Phys. Rev. Lett. 49 (1982) 259.
[3] P. Baillon et al., Nuovo Cim. 3 (1967) 393.
[4] C. Amsler et al., Phys. Lett. B 358 (1995) 389.
[5] T.A. Armstrong et al., Z. Phys. C 52 (1991) 389.
[6] A. Bertin et al., Phys. Lett. B 361 (1995) 187.
[7] Z. Bai et al., Phys. Rev. Lett. 65 (1990) 2507.
[8] J.E. Augustin et al., Phys. Rev. D 46 (1992) 1951.
[9] Review of Particle Physics, R.M. Barnett et al., Phys. Rev. D 54 (1996) 361.
[10] A. Palano, Proc. of the NATO Advanced Study Institute on Hadron Spectroscopy and the Confinement Problem, ed. D.V. Bugg, London 1995, p. 189.
[11] S.U. Chung, Proc. Hadron'95, eds. M.C. Birse, G.D. Lafferty and J.A.Mc Govern, Manchester 1995, p. 19.
[12] F. Nichitiu, Proc. Hadron'95, eds. M.C. Birse, G.D. Lafferty and J.A.Mc Govern, Manchester 1995, p. 164.
[13] A. Kirk, Proc. Hadron'95, eds. M.C. Birse, G.D. Lafferty and J.A.Mc Govern, Manchester 1995, p. 127.
[14] A. Lanaro, Invited talk to LEAP'96, Dinkelsbühl, Germany.
[15] D. Alde et al., Preprint IHEP 96-39 (1996).
[16] M. Sosa et al., Proc. Hadron'95, eds. M.C. Birse, G.D. Lafferty and J.A.Mc Govern, Manchester 1995, p. 408.
[17] A. Adamo et al., Sov. J. Nucl. Phys. 55 (1992) 173.
[18] G.C. Bonazzola et al., Nucl. Instr. Meth. A 356 (1995) 270.
[19] A. Bertin et al., Phys. Lett. B 385 (1996) 493.
[20] S.M. Flattè, Phys. Lett. B 63 (1976) 224.
[21] J.H. Lee et al., Phys. Lett. B 328 (1994) 227.
[22] D. Aston et al., Nucl. Phys. B 296 (1988) 493.
[23] L. Rosselet et al., Phys. Rev. D 15 (1977) 574.
[24] Review of Particle Physics, R.M. Barnett et al., Phys. Rev. D 54 (1996) 349.
[25] S.U. Chung et al., Ann. Physik 4 (1995) 404.
[26] K.D. Duch et al., Z. Phys. C 45 (1989) 223.
[27] Yu.D. Prokoshkin and S.A. Sadovsky, contribution to LEAP'96, Dinkelsbühl, Germany.
[28] M.R. Pennington, Proc. Hadron'95, eds. M.C. Birse, G.D. Lafferty and J.A.Mc Govern, Manchester 1995, p. 3.
[29] M.A. Shifman et al., Nucl. Phys. B 147 (1979) 385, 448, 519.
[30] G. Bali et al., Phys. Lett. B 309 (1993) 378.
[31] D. Weingarten, Nucl. Phys. B 34 (1994) 29.
[32] I. Kitamura et al., Nuovo Cim. A 107 (1994) 2429.
[33] R.L. Jaffe and K. Johnson, Phys. Lett. B 60 (1976) 201.
[34] M. Chanowitz and S. Sharpe, Nucl. Phys. B 322 (1983) 211.
[35] Ph. Gaville et al., Z. Phys. C 16 (1982) 119.
[36] J.J. Becker et al., Rev. Lett. B 59 (1987) 186.
[37] D.O. Caldwell, Proc. Int. Conf. on Hadron Spectroscopy, Ajaccio (1989), ed. Frontières.
[38] S.I. Bityukov et al., Phys. Lett. B 203 (1988) 327.
[39] C.E. Carlson et al., Phys. Rev. D 30 (1984) 1594.
[40] S. Ishida et al., Prog. Theor. Phys. 82 (1989) 119.
[41] J. Weinstein and Isgur, Phys. Rev. D 27 (1983) 588; D 41 (1990) 2236.
[42] R.S. Longacre, Phys. Rev. D 42 (1990) 874.